Theoretical Calculations of Pressure Broadening Coefficients for H_2O Perturbed by Hydrogen or Helium Gas

Robert R. Gamache

and

James B. Pollack

Final Report

Contract No. NCC2-5029

January 1995

Prepared for

NASA-Ames University Consortium
c/o Eleanor Figueroa
Mail Stop 223-9
Moffett Field, CA 94035-1000

TABLE OF CONTENTS

LIST OF TABLES

LIST OF FIGURES

ABSTRACT

Halfwidths were calculated for H_2O with H_2 as a broadening gas and were estimated for He as the broadening species. The calculations used the model of Robert and Bonamy with parabolic trajectories and all relevant terms in the interaction potential. The calculations investigated the dependence of the halfwidth on the order of the atom-atom expansion, the rotational states, and the temperature in the range 200 to 400K. Finally, calculations were performed for many transitions of interest in the 5 μm window region of the spectrum. The resulting data will be supplied to Dr. R. Freedman for extracting accurate water mixing ratios from the analysis of the thermal channels for the Net Flux experiment on the Galileo probe.

1.0 INTRODUCTION

The atmospheres of the giant planets are made mostly of H_2 and He, the same constituents that are the dominant atomic constituents of the Sun. This composition reflects the ability of the massive giant planets to have gravitationally captured large amounts of gases from their birthplace in the primordial soar nebula as well as solids (e.g., water) that were eventually volatilized into heavier gases in their atmospheres. In contrast, the terrestrial planets, such as Earth and Venus, contain atmospheric gases derived almost exclusively from the solid component of the solar nebula. By obtaining accurate estimates of the water abundance in the atmospheres of the giant planets, we will be able to place important constraints on the relatively efficiency with which they accumulated gases and solids from the primordial solar nebula.

There are selected regions of the thermal infrared spectrum of the giant planets, especially Jupiter, that are known to contain water vapor features. One example is a portion of the so-called 5 micron "window". However, when viewed from space, much of the emission comes from altitude regions that are cold enough for water to follow approximately its saturation vapor pressure curve and what is needed is its abundance in the hotter, well mixed region below the water clouds. The Net flux experiment (NFR) on the Galileo probe contains several broad band channels that encompass water features and it will obtain data below the water condensation region. Such measurements will be made during the descent of the Galileo probe (built under the leadership of NASA Ames) in early December, 1995. Ames collaborator James B. Pollack is a Co-

Investigator on the NFR experiment and is responsible for analyzing the thermal channels of the NFR, including the ones containing water features.

In order to retrieve accurate estimates of water mixing ratio from these data, it is essential that all relevant spectroscopic parameters of the relevant water lines be well known. The data for the molecular absorption parameters are that of Rothman *et al.* (1) The molecular absorption data for each spectral transition (line) consist of at least the resonant frequency, line intensity, air-broadened halfwidth, and lower state energy. In addition HITRAN (1) also contains the temperature dependence of the air-broadened halfwidth, weighted transition moment squared, self-broadened halfwidth, line shift, quantum identification of the transition and some error and reference codes. While the line strengths and energy levels are relatively well known, the pressure broadening half widths have major uncertainties in them (at least a factor of several) that would limit water abundance determinations severely. In particular, there is a gross inadequacy in what the halfwidths are when H_2O is being broadened by H_2 and what the temperature dependence of this half width are. A similar situation exist for water broadening by He, although estimates are acceptable here because H_2 broadening dominates. The temperatures of interest are centered around room temperature and range from 200 K to 400 K. The pressures of interest are centered around 5-10 bars and range from 1 to 20 bars. (2-4)

The effect of errors in the halfwidth on retrieved profiles has been systematically investigated (5) with the conclusion that inaccurate collision-broadened halfwidth values lead to significant errors in retrieved profiles. For the atmospheres of giant planets, such as Jupiter, the broadening by H_2 and He must be known.

Only two measurements (6-7) of hydrogen-broadened halfwidths of water vapor have been made. These were for the 22 GHz line of water vapor (6 1 6 ← 5 2 3). To our knowledge there have been no theoretical calculations. For He-broadening there has been slightly more work (6-11) with a total of 11 lines having been measured and the temperature dependence considered for some of the lines. (8-11) This will allow a ratio of H_2 to He broadening to be estimated.

There are 4 dominant bands of water vapor in the 5μm region (≈ 2000 cm^{-1}); (010), (100), (020), and (001). Although the Watson constants are known for these bands (12) the initial calculations of the wavefunctions and energies for the states will consider the ground vibration state only. This has been shown to introduce little error (13) in the determination of the halfwidth for vibrational bands with only a few quanta of energy. The parameters for the trajectory dynamics for the H_2O-H_2 system were determined. Calculations of halfwidth were performed for the lower state rotational quantum numbers, J" and Ka", varying from 0 to 13 and 0 to 8, respectively. The temperature dependence of the halfwidths was studied over a range from 200-400 K. The results of these calculations were compared with the experimental values.

Different methods to estimate the halfwidths for transitions not considered in this study were investigated. Finally, we determine a method for estimating halfwidth values for He-broadening of water vapor using the measured or calculated values for other perturbing species. While there are limitations on such a method, it does allow a guess at the He-broadened values which may not be as critical due to the lesser amount of this gas in the atmospheres of the planets.

The database of broadening coefficients will be used by Dr. J. Pollack for extracting accurate water mixing ratios from the analysis of the thermal channels for the Net Flux experiment on the Galileo probe. It is expected that these broadening parameters will greatly improve the accuracy of the results.

2.0 THEORETICAL CALCULATIONS

The theoretical calculations made here are based on a fully complex implementation of the theory of Robert-Bonamy (14) (RB). Previous attempts at the (Real valued) formalism applied to asymmetric rotor molecules (15-17) contained errors in the development of the atom-atom potential coefficients. These were corrected (18) and some inconsistencies in previous calculations (19) explained. The formalism presented here is slightly different from Ref. 18 in that a more manageable expression is employed for the atom-atom potential allowing more complete expansions to be considered. A major difficulty in the RB method has been evaluating Fourier-Laplace transforms of correlation functions, which arise in the theory because of the semiclassical treatment of translational motion. Computer-assisted algebraic methods have proved very useful in addressing this. Emphasis throughout is placed on generality, insofar as the formulas are complex-valued (yielding line shifts as well as widths) and for the most part suitable for any pair of colliding molecules.

The intermolecular potential appears in the theory as a spherical tensor expansion in the intermolecular separation R,

$$V^{(R\text{-frame})}(t) = \sum_{\substack{\vec{lm} \\ mq}} v\vec{lm}\,mq\, \frac{D^{l_1}_{mm_1}(\Omega_1)\, D^{l_2}_{-m-m_2}(\Omega_2)}{R^q} \qquad (1)$$

4

The D's are components of spherical tensors (Wigner rotation matrices (20))
as given by Gray. (21) Symbols Ω_1 and Ω_2 specify the orientation of the
molecule-fixed frame within the conventional "R-frame". (22) Coefficients
$\vec{v}_{lm\,mq}$ depend on how the molecules are situated within the molecule-fixed
frame. In the present calculations, water vapor is taken in the I^R
representation (23) and N_2 lies along the z-axis.

The radial parts of Eq. (1) are not the most general form, but suffice
to describe both electrostatic and atom-atom Lennard-Jones interactions.
The electrostatic potential is the usual expansion (21-22) of the charge
distribution in terms of the electric moments of the molecules, e.g. dipole-
dipole, dipole-quadrupole, etc.

$$V^{elec}_{1,2} = V_{\mu_1\mu_2} + V_{\mu_1\theta'_2} + V_{\theta'_1\mu_2} + V_{\theta''_1\mu_2} + V_{\theta'_1\theta'_2} + V_{\theta''_1\theta'_2} + \dots . \qquad (2)$$

Here the contributing terms are the dipole(H_2O)-quadrupole(H_2) and
quadrupole(H_2O)-quadrupole(H_2) interactions. The values of the dipole
and quadrupole moment components of H_2O were taken from Ref. 24 and
the quadrupole moment of H_2 was taken from Ref. 25. In the derivation of
atom-atom coefficients, it is convenient to define an order Q of the atom-
atom expansion as

$$Q=(q-q_0) \qquad (2)$$

with q_0 typically 6 or 12. In previous formulations, expressions for
anisotropic atom-atom coefficients $\vec{v}_{lm\,mq}$ have been obtained explicitly to
order Q=4, using for example the algebraic method of Labani et al. (15-17)
The orders required here, Q=8 or more, are high enough to make that
method cumbersome, even with computer assistance.(18) Therefore we
use the expressions derived by Sack (26) and Downs et al. (27) (see also

5

Gray (21)), repeated in the Appendix in slightly modified form as Eq. (A.1). A static, zero-rank expansion of the atom-atom potential (l_1 and l_2 both zero) defines the isotropic potential used to compute the translational motion of the molecules.

The expression for the half width coefficient at half height in RB theory is

$$\phi_{if} = (\gamma_{if} - i\delta_{if}) = \frac{n_2}{2\pi c p} \sum_2 \rho_2 \int_0^\infty v f(v) \, dv \int_0^\infty 2\pi b \, S_{if}(b,v,J_2) \, db \qquad (6)$$

where v is the relative velocity of the two molecules, b the impact parameter, n_2 the number density of the perturber gas, and p the pressure. The observed half width is assumed to be a linear function of pressure, $\phi_{if}^{obs} = p\phi_{if}$. We assume the mean relative thermal velocity approximation, replacing the Maxwell-Boltzmann distribution $f(v)$ by $\delta(v-\bar{v})$, where $\bar{v}$ is the average relative velocity. The interruption function, S_{if}, is given by

$$S_{if}(b,v,J_2) = 1 - e^{-\left(\overset{\bullet}{S}_{2,i2} + S_{2,f2} + S_{2,f2i2} + \overset{\bullet}{S}_{1,i} + S_{1,f}\right)} \qquad (7)$$

The components $S_{2,i2}$, etc., are complex-valued analogs of terms familiar from ATC (28-29) theory. Both "outer" terms $S_{2,i2}$ and $S_{2,f2}$ and "middle" term $S_{2,f2i2}$ are expressed in terms of resonance functions F and reduced Liouville matrix elements D,

$$S_{2,i2} = \frac{1}{\hbar^2 [J_i][J_2]} \sum_{i',2'} \sum_{\overrightarrow{lm^a m^b}} D^{\overrightarrow{lm^a m^b}}_{ii,i'i'} \; F^{\overrightarrow{lm^a m^b}}_{22,2'2'}(\omega) \tag{8}$$

$$S_{2,f2i2} = \frac{-2}{\hbar^2 [J_2]} \sum_{2'} \sum_{\overrightarrow{lm^a m^b}} D^{\overrightarrow{lm^a m^b}}_{if,if} \; F^{\overrightarrow{lm^a m^b}}_{22,2'2'}(\omega) \; (-)^{J+J_i+J_f+l_i} \begin{Bmatrix} J_i & J_i & l_1 \\ J_f & J_f & J \end{Bmatrix} \tag{9}$$

where $S_{2,f2}$ is obtained from Eq. 8 by the substitutions i->f and i'->f'. We use the notation $[J] \equiv 2J+1$, $\overrightarrow{m^a} \equiv m^a_1, m^a_2$ etc., and {:::} indicates a Racah coefficient. Complex-valued expressions for F and D suitable for any molecular pair are given in the Appendix.

The exponential form of Eq. (7) comes about as a result of a cumulant formulation of the perturbation expansion for the collision. (30) Because of it, imaginary parts of S affect not only the shift, but the width as well, an effect not achieved in ATC theory.

As stated above, some difficulty arises in the evaluation of the integrals over translational degrees of freedom, Eq. (A.8), because of the large orders and tensorial ranks required. In the appendix we describe a computer-assisted method for finding the real parts of Eq. (A.8) in the parabolic approximation of RB. Imaginary parts of S_2 were initially obtained by numerical integration of the intermolecular equations of motion, but found to be insignificant compared to the contribution of S_1 obtained by Eq. (4). Therefore only the real parts of S_2 are calculated according to the parabolic approximation. Techniques for evaluating the fully complex integrals in the parabolic approximation are described elsewhere. (31)

3.0 CONVERGENCE OF THE INTERMOLECULAR POTENTIAL

Values of electrostatic moments for H_2O and H_2 are given in Table I.
The Lennard-Jones parameters necessary for the atom-atom component of
the potential can be determined by fitting virial data (32) or by using
combination rules. Because of a lack of virial data for the H_2O-H_2 system,
combination rules (22) were used to obtain hetero-atomic Lennard-Jones
parameters (ε_{HN}, σ_{HN}, etc.) from homo-atomic ones quoted by Bouanich (32)
(ε_{HH}, σ_{HH}, etc.), with results given in Table II. The isotropic Lennard-Jones
parameters ε_{iso} and σ_{iso}, are derived from these atom-atom parameters by
formal expansion. No attempt has been made to optimize them to improve
the match with experimental line widths, although such adjustments would
certainly be justified considering their probable uncertainties.

For the atom-atom interaction, there is the concern of convergence
with respect to the order $Q=(q-q_0)$. Within the present perturbative
framework, higher values of Q correspond to smaller intermolecular
separations. Therefore convergence of calculated line widths with respect
to Q carries information about the intermolecular distances involved. For
systems with weak electrostatic moments higher orders of Q become
necessary. Convergence results are displayed in Fig. 1 for the 22 GHz
transition at 293 (open circles) and 300 K (solid squares). Plotted are the
calculated halfwidth versus the order Q used in the calculation clearly
demonstrating that orders of at least Q=8 are required for satisfactory
convergence. These observations suggest a large role played by the closest
range (repulsive) part of the atom-atom potential which is expected for
this system given the value of the quadrupole moment of H_2. This effect

has been discussed in a study (33) of CH_4 in collision with N_2. In the calculations that follow, the order of Q has been set to 8 with maximum values of l_1 and l_2 set at 2.

All transitions for the principal isotopic species of water vapor in the region 1500-2500 cm^{-1} were selected from the HITRAN database.(1) This resulted in 2356 transitions. From this group, transitions with an intensity greater than 1. $x10^{-23}$ cm^{-1}/molecule cm^{-2} and J" $\leq$ 13 were selected. Because the calculations neglect the vibrational dependence, only lines with unique sets of rotational quantum numbers were retained. (Note, the interchange of the upper and lower quantum numbers was considered.) This gave a list of 377 transitions which was expanded to consider a greater range of Ka" values yielding 626 transitions for this spectral region. Calculations were made for these transitions of water vapor at T=296K. The results of the calculations are in Table III.

Calculations were also made for the 22 GHz line of water vapor at 293 and 300 K to compare with the measurements of Liebe and Dillon (6) and Kasuga et al. (7) These are compared with the experimental measurements in Table IV.

4.0 ESTIMATED HALFWIDTHS

The halfwidths of some 626 transitions of water vapor were calculated. For application to radiative transfer studies all the lines of significant absorption within the spectral range must be known. Since one is dealing with large optical paths, even weak optical transitions must be accounted for. For a typical atmospheric path length of 10 km with 2%

H_2O, transitions with integrated intensities greater than about 10^{-27} $cm^{-1}/(molecule \cdot cm^{-2})$ have to be accounted for according to a 1% transmission at line center criterion. This roughly leads to lower state energies, for lines of the rotational band, up to 4500 cm^{-1} and J and Ka quantum numbers up to 20 and 15, respectively. Hence there is a need to approximate the halfwidths for the transitions that have not been studied.

Because previous works only provided the H_2-broadened halfwidth for the 22 GHz line of water vapor values for all other transitions could only be guessed at. This is usually done (34-35) by scaling values derived for some other perturbing species such as N_2 or air. Such procedures can only yield approximate values for transitions where the halfwidth for another perturbing species is known. Often default values must be used. Better estimates of the halfwidth are provided by the procedure described below.

Two different methods for estimating halfwidths were considered First, a simple average of the halfwidth as a function of $(J''+J')/2$ was made. Second, a polynomial in J'' and Ka'' was used to fit the calculated halfwidths. The polynomial expression employed by Gamache et al. (36) was used

$$\gamma(poly) = b_0 + b_1 * \left(\frac{J''+J'}{2}\right) + b_2 * \left(\frac{J''+J'}{2}\right)^2 + b_3 * \left(\frac{Ka''+Ka'}{2}\right). \tag{9}$$

The coefficients were obtained by least-squares fitting to the calculated data resulting in the following coefficients; $b_0 = 0.098\ 096$, $b_1 = -0.409\ 31\ 10^{-2}$, $b_2 = 0.120\ 91\ 10^{-3}$, and $b_3 = 0.553\ 12\ 10^{-3}$.

The halfwidths from the averaging procedure and from the polynomial were compared with the calculated results. The average

percent difference (APD), the average absolute percent difference (AAPD), and the minimum and maximum percent differences were calculated as a function of (J"+J')/2. The AAPD for all the lines studied is 5.3% for both methods and the maximum and minimum percent differences are 13 and -22% for the averaging method and 12 and -25% for the polynomial method. In Fig. 2 the percent difference versus (J"+J)/2 is plotted for the averaging method (dots) and the polynomial method (+ symbol). Note the polynomial results are shifted on the (J"+J)/2 axis in order to better compare the methods. The figure gives an estimation of the range of error one might expect when using the methods to predict halfwidths that have not been calculated. The AAPD results indicate that both methods are quite similar. Because the polynomial is limited to only the fit range, the results are similar, and for speed of calculation, the averaging method is recommended for determining halfwidths not listed in Table III.

5.0 TEMPERATURE DEPENDENCE OF THE HALFWIDTHS

The temperature dependence of the halfwidths was considered. Twenty transitions from J"=1 to 9 and Ka"=0 to 7 were chosen to study the structure of the temperature exponent as a function of J" and Ka". Calculations of the halfwidth were made at the temperatures 200, 250, 296, and 400 K. The temperature dependence of the halfwidth is taken as (37)

$$\gamma(T) = \gamma(T_0) \left(\frac{T_0}{T}\right)^n ,$$

(11)

where the reference value (T_0) was taken at 296K, however changing the reference temperature has no effect on the results. The calculated halfwidths at the four temperatures studied were fit to Eq. (1) to give the temperature exponent, n, and the correlation coefficient of the fit. The resulting correlation coefficients indicated Eq. (11) was valid to describe the temperature dependence in the range considered. The calculated temperature exponents are given in Table V. Figure 3 displays the variation of n as a function of the initial rotational state quantum numbers and Figure 4 is the temperature exponent versus Ka" for the transitions with J"=5. The temperature exponents are transition dependent and range roughly from 0.3 to 0.6. From Figs. 3 and 4, it can be concluded that it is difficult to predict the temperature exponent of a particular transition based on the n values from other transitions.

6.0 DISCUSSION

Table IV is a comparison of the 8th order calculations with the measurements of Liebe and Dillon (6) and Kasuga et al. (7) for the 22 GHz line of water vapor. The measurement of Liebe and Dillon was made at 300 K with a reported uncertainty of 2.5%. The work of Kasuga et al. was done at 293 K with an uncertainty of 11% for H_2-broadening. It is worth noting that the measurements do not display the proper temperature dependence even if the uncertainties are considered. These measurements imply a temperature exponent of -0.15 compared with the calculated value of 0.47 and a kinetic theory value of 0.5. The calculated value at 300 K shows very good agreement (< 1%) with the measurement of Liebe and

Dillon, (6) however the value calculated at 293 K compared with the value of Kasuga et al. (7) shows a -20% error. The problem noted in the measurements make them difficult to use as a gauge for the reliability of the calculations.

The RB theory employed in these calculations of halfwidths for H_2O may have several short comings. Although the atom-atom potential was carried to 8th order, Fig. 1 suggest that there are small contributions from higher order. The current theory is expected to be more suspect as the energy gap between collisional states increases. This varies as a functions of the rotational state and as J" increases the uncertainty of the calculation will also increase. The calculations employed only the real part of the interruption functions, however for a ground state calculation this should not add significant uncertainty. For transitions with $J \leq 6$ an average uncertainty of ±5% with maximum uncertainty less than 15-20% might be expected. The transitions with $J > 6$ considered here should have an average uncertainty less than ±10% with maximum uncertainty less than 35%. These values should be taken only as an estimate for error analysis.

The theory of Robert and Bonamy only considers the first term in the expansion of the density and as such will not be applicable to pressures greater than a few bars. Also the theory only considers the diagonal term in the relaxation matrix (38) thus the effects of line mixing are neglected as well. These calculations are however the first step in understanding the line shape for H_2O in collisions with H_2.

7.0 He-BROADENING OF H₂O

In Table VI the measured values of the He-broadened halfwidth of water vapor are presented for all transitions studied.   When available the temperature coefficient is also given.   With this data we can form ratios to halfwidths for other perturbing species in order to estimate the He-broadened values.   Because of the rather large uncertainties and the temperature of the study of Ref. (11), the last seven entries in the table, these data will not be considered in the analysis.   Table VII gives the three remaining transitions for He-broadened data and the coresponding halfwidth and ratio with other broadening species.   The experimental data of Table VI has been corrected to 296 K using the temperature exponents listed in the table.   The rotational state quantum numbers (upper and lower) are labeled 1, 2, and 3 in Table VII and correspond to the transitions 3 1 3←2 2 0,4 4 1←3 2 1, and 6 1 6 ←5 2 3 respectively.   All ratios are the He-broadened value divided by the value for the particular perturbing species and all halfwidths are in units of cm^{-1}/atm at 296K. Other values in the table are calculated values from Ref. (39) for N_2- and O_2-broadening, from Ref. (36) for CO_2-broadening, and from this work for H_2-broadening.   The ratios show roughly a 30% variation.   Given this and the few lines considered the uncertainty of 50% might be assigned in the scaled He-broadened values.

8.0 SUMMARY

A database of H_2-broadened halfwidths of water vapor transitions were calculated with particular interest for the 5 μm "window" region. A total of 626 transitions were studied for rotational states of H_2O from $J"=0$ to 13 and Ka=0 to 8. Comparison with two measurements display both good and poor agreement, however the measurements do not appear to be in agreement with each other unless the temperature exponent is negative. Thus, there differences in the measurements that are yet to be explained. The temperature dependence of the halfwidth was calculated for 20 transitions from $J"=1$ to 9. In order to better assess the reliability of these calculations it is suggested that measurements be made on a number of transitions studied in this work and the temperature dependence studied for several transitions.

The data calculated in this report will be delivered to R. Freedman for use in the reduction of the NFE data.

A manuscript on this work is being prepared for submission to a refereed journal.

9.0 REFERENCES

1. L. S. Rothman, R. R. Gamache, A. Goldman, L. R. Brown, R. A. Toth, H. M. Pickett, R. L. Poynter, J.-M. Flaud, C. Camy-Peyret, A. Barbe, N. Husson, C. P. Rinsland and M. A. H. Smith, "The HITRAN database: 1986 edition," *Appl. Opt.* **26**, 4058 (1987).

2. D. Gautier and T. Owen, "The composition of outer planet atmospheres". In "Origin and Evolution of Planetary and Satellite Atmospheres", eds. S. K. Atreya, J. B. Pollack, and M. S. Matthews (Univ.. Arizona Press, Tucson, pp. 487-512, 1989.

3. J. B Pollack and P. Bodenheimer, 1989. "Theories of the origin and evolution of the giant planets", In "Origin and Evolution of Planetary and Satellite Atmospheres", eds. S. K. Atreya, J. B. Pollack, and M. S. Matthews (Univ.. Arizona Press, Tucson, pp. 564-602..

4. L. A. Sromovsky, F. A. Best, H. E. Revercomb, and J. Hayden, Space Sci. Rev.60, 233-262, (1992).

5. M. A. H. Smith and L. L. Gordley, J. Quant. Spectrosc. Radiat. Transfer 29, 413 (1983); B. Kivel, H. E. Fleming and W. G. Planet, *J. Quant. Spectrosc. Radiat. Transfer* **17**, 181 (1977).

6. H. J. Liebe and T. A. Dillon, J. Chem. Phys. **50**, 727-732, (1969).

7. T. Kasuga, H. Kuze, and T. Shimizu, J. Chem. Phys. **69**, 5195-5198 (1978).

8. J. R. Izatt, H. Sakai, and W. S. Benedict, J. Opt. Soc. Am. **59**, 19-26, (1969).

9. M. Godon, and A. Bauer, Chem. Phys. Lett. **147**, 189-191, (1988).

10. T. M. Goyette, and F. C. De Lucia, J. Mol. Spectrosc. **143**, 346-358, (1990)

11. J. R. Izatt, H. Sakai, and W. S. Benedict, J. Opt. Soc. Am. **59**, 19-26, (1969).

12. J.-M. Flaud and C. Camy-Peyret, private communications, 1990.

13. R. R. Gamache, J.-M. Hartmann, and L. Rosenmann, J. Quant. Spectrosc. Radiat. Transfer **52**, 481-499 (1994).

14. D. Robert and J. Bonamy, J. Phys. (Paris) 40, 923-943 (1979).

15. B. Labani, J. Bonamy, D. Robert, J. M. Hartmann and J. Taine, J. Chem. Phys. 84, 4256-4267 (1986).

16. J. M. Hartmann, J. Taine, J. Bonamy, B. Labani and D. Robert, J. Chem. Phys. **86**, 144 (1987).

17. B. Labani, J. Bonamy, D. Robert, and J. M. Hartmann, J. Chem. Phys. **87**, 2781 (1987).

18. S. P. Neshyba, and R. R. Gamache, J. Quant. Spectrosc. Radiat. Transfer **50**, 443-453, 1993.

19. S. Bouazza, A. Barbe, J. J. Plateaux, L. Rosenmann, J.-M. Hartmann, C. Camy-Peyret, J.-M. Flaud, and R. R. Gamache, J. Mol. Spectrosc. **157**, 271-289, 1993.

20. U. Fano and G. Racah, *Irreducible Tensorial Sets* (Academic Press, Inc., New York 1959).

21. C. G. Gray and K. E. Gubbins, *Theory of Molecular Fluids, vol. I* (Clarendon Press, Oxford 1984).

22. J. O. Hirschfelder, C. . Curtiss, and R. B. Bird, *Molecular Theory of Gases and Liquids* (John Wiley and Sons, Inc., New York 1954).

23. H. C. Allen, Jr. and P. C. Cross, "*Molecular Vib-Rotors: The Theory and Interpretation of High Resolution Infrared Spectra*," J. Wiley, NY 1963.

24. S. L. Shostak and J. S. Muenter, J. Chem. Phys. **94**, 5883-5890 (1991); J. Verhoeven and A. Dymanus, J. Chem. Phys. **52**, 3222-3233 (1970).

25. J. D. Poll and L. Wolniewicz, J. Chem. Phys. **68**, 3053-3058 (1978).

26. R. A. Sack, J. Math. Phys. **5**, 260 (1964).

27. J. Downs, C. G. Gray, K. E. Gubbins, and S. Murad, Mol. Phys. **37**, 129 (1979).

28. P. W. Anderson, Phys. Rev. 76, 647-661 (1949); 80, 511-513 (1950).

29. C. J. Tsao and B. Curnutte, Jr., J. Quant. Spectrosc. Radiat. Transfer 2, 41-91 (1962).

30. R. Kubo, J. Math. Phys. **4**, 174 (1963).

31. R. Lynch, Ph.D. dissertation, Physics Department, University of Massachusetts Lowell (in progress).

32. J.-P. Bouanich, J. Quant. Spectrosc. Radiat. Transfer, **47** 243-250 (1992).

33. S. P Neshyba, R. Lynch, R. R. Gamache, T. Gabard and J.-P. Champion, J. Chem. Phys. **101**, 9412-9421 (1994).

34. D. Crisp, D. A. Allen, D. H. Grinspoon, and J. B. Pollack, *Science* **253**, 1263 (1991).

35. J. B. Pollack J. B. Dalton, D. Grinspoon, R. B. Wattson, R. Freedman, D. Crisp, D. A. Allen, B. Bezard, C. DeBergh, L. P. Giver, Q. Ma, and R. Tipping, Icarus **103**, 1-42 (1993).

36. R. R. Gamache, S. P Neshyba, J. J. Plateaux, A. Barbe, L Régalia, and J. B. Pollack, "CO_2-Broadening of Water-Vapor Lines," J. Mol. Spectrosc., in press, 1995.

37. R. R. Gamache, J. Mol. Spectrosc. **114**, 31-41 (1985); R. R. Gamache and L. S. Rothman, J. Mol. Spectrosc. **128**, 360-369 (1988).

18

38. A. Ben-Reuven, "Spectral Line Shapes in Gases in the Binary Collision Approximation," in Adv. Chem Phys. **33**, 235-293 (1975).

39. R. R. Gamache, unpublished results, 1994.

40. W. H. Press, B. P. Flannery, S. A. Teukolsky, and W. T. Vetterling, *Numerical Recipes, The Art of Scientific Computing* (Cambridge University Press, Cambridge, 1986).

41. *Handbook of Mathematical Functions*, M. Abramovitz and I. Stegun, eds. (Dover 1972).

APPENDIX

Coefficients of the atom-atom potential are given by (26-27)

$$v^{\overrightarrow{lm}}_{nq} = A\ B \tag{A.1a}$$

with

$$A = (-1)^{l_2}\sqrt{\frac{(4\pi)^2}{(2l_1+1)(2l_2+1)}}\ \frac{1}{\left(\frac{1}{2}\right)_{l_1}\left(\frac{1}{2}\right)_{l_2}}\ \sum_{l=|l_1-l_2|}^{l_1+l_2}\left(\frac{q_0}{2}\right)_\Lambda\left(\frac{q_0-1}{2}\right)_\lambda\left(\Lambda+\frac{q_0}{2}\right)_w\left(\lambda+\frac{q_0-1}{2}\right)_w$$

$$C(l_1\ l_2\ l;\ 0\ 0\ 0)\ C(l_1\ l_2\ l;\ m\ -m\ 0) \tag{A.1b}$$

and

$$B = \sum_{\alpha\beta} d_{\alpha\beta}(q_0)\ Y^*_{l_1m_1}(\omega_\alpha)\ Y^*_{l_2m_2}(\omega_b)\ \sum_{z=-w}^{w,2}\frac{r_\alpha^{l_1+w+z}\ r_\beta^{l_1+w-z}}{\left(l_1+\frac{3}{2}\right)_{\frac{w+z}{2}}\left(l_2+\frac{3}{2}\right)_{\frac{w-z}{2}}\left(\frac{w+z}{2}\right)!\left(\frac{w-z}{2}\right)!} \tag{A.1c}$$

,

where $(...)_\lambda$ is a displaced factorial. (27) In Eq. (1) in the text, the sum over variable q is implicitly defined by

$$q=(q_0+Q),\ Q=l_1+l_2+2w \tag{A.2}$$

Reduced matrix elements in $S_{2,i2}$ are given by

$$D^{\overrightarrow{lm^am^b}}_{\substack{ii,i'i'\\22,2'2'}} = <i\|D^{l_1}_{*,m_1^1}\|i'><i\|D^{l_1}_{*,m_1^1}\|i'>^*<2\|D^{l_2}_{*,m_2^2}\|2'><2\|D^{l_2}_{*,m_2^2}\|2'>^* \tag{A.3}$$

Reduced matrix elements in $S_{2,f2i2}$ are given by

$$D^{\overrightarrow{lm^a m^b}}_{22,2'2'} = \; <i\|D^{l_1}_{*,m_1^b}\|i><f\|D^{l_1}_{*,m_1^a}\|f>^* <2\|D^{l_2}_{*,m_2^b}\|2'><2\|D^{l_2}_{*,m_2^a}\|2'>^* \quad (A.4)$$

Reduced Hilbert-space matrix elements appearing above are defined by

$$\left\langle J_i \tau_i M_i \left| D^{l}_{m'm} \right| J_{i'} \tau_{i'} M_{i'} \right\rangle \equiv (-)^{M_i + J_i} \begin{pmatrix} J_i & J_{i'} & l \\ M_i & -M_{i'} & -m \end{pmatrix} \left\langle J_i \tau_i \left\| D^{l}_{*m} \right\| J_{i'} \tau_{i'} \right\rangle \quad (A.5)$$

Complex-valued resonance functions are given by

$$F^{\overrightarrow{lm^a m^b}}(\omega) = \frac{1}{[l_1][l_2]} \sum_{\substack{m' \\ n^{a,b} q^{a,b}}} \left(v^{\overrightarrow{lm^a} n^a q^a} \right)^* \left(v^{\overrightarrow{lm^b} n^b q^b} \right) g^{\overrightarrow{lm} n^a n^b q^a q^b}(\omega) \quad (A.6)$$

The sum over m' comes about from the transformation from R-frame Euler angles (Ω) of Eq. (1) to laboratory frame angles (θ). Requiring intermolecular motion in the x-z plane,

$$\Omega = \Psi\Theta, \; \Psi = (0,\psi,0) \quad (A.7)$$

leads to

$$g^{\overrightarrow{lm} n^a n^b q^a q^b} = \mathcal{F}\left(\left\{ \frac{d^{l_1}_{n^a m'_1}(\psi)\, d^{l_2}_{-n^a m'_2}(\psi)}{R^{qa}} \right\}, \left\{ \frac{d^{l_1}_{n^b m'_1}(\psi)\, d^{l_2}_{-n^b m'_2}(\psi)}{R^{qb}} \right\} \right) \quad (A.8)$$

where $\mathcal{F}$ is the Fourier Laplace transform of a correlation function

$$\mathcal{F}(a,b) \equiv \int_0^\infty e^{i\omega t} dt \int_{-\infty}^\infty a^*(t'-t)\, b(t')\, dt \qquad (A.9)$$

Real parts of $\mathcal{G}$ are expressed as products

$$\mathcal{R}e\left(\mathcal{G}^{\overrightarrow{lm}\, n^a n^b q^a q^b}(\omega)\right) = (1/2)\, g^{\overrightarrow{lm'}\, n^a q^a\, *}(\omega)\, g^{\overrightarrow{lm'}\, n^b q^b}(\omega) \qquad (A.10)$$

where

$$g^{\overrightarrow{lm'}\, nq}(\omega) = \int_{-\infty}^\infty dt\; e^{i\omega t}\, \frac{d^{l_1}_{nm'_1}(\psi)\, d^{l_2}_{-nm'_2}(\psi)}{R^q} \qquad (A.11)$$

In practice, tensors d^l_{mn} are represented as sums of the form

$$d^l_{mn}(\psi) = \sum_j t_j \sin^{s_j}(\psi) \cos^{c_j}(\psi). \qquad (A.12)$$

Computer representation of these sums is accomplished via FORTRAN structures, in which we keep track of values of t_j, s_j, and c_j for each function d^l_{mn}. Products $d^l_{mn} \times d^{l'}_{m'n'}$ appearing in Eq. (A.11) are represented as the same structure, using a heapsort algorithm (40) to collect like values of s_j, and c_j and thereby compress the representation. As the RB parabolic approximation ($\sin(\psi)=v_c t/R(t)$, etc.) honors the identity $\cos^2+\sin^2=1$ only to second order in time, final relations using the approximation are not unique. We employ the substitution $\cos^2=1-\sin^2$ in product structures $d^l_{mn} \times d^{l'}_{m'n'}$ for all entries in which $c_j > 1$. After these manipulations, Eq. (A.11) is expressed as a sum of terms of the form

$$f_v^m(\omega) = \int_{-\infty}^{\infty} e^{i\omega t} \frac{t^m}{(1+t^2)^{v+1/2}} dt \qquad (A.12)$$

which have the formal solution

$$f_v^m(\omega) = \frac{2(-i)^m}{(2v-1)!!} \left(\frac{\partial}{\partial\omega}\right)^m \left\{\omega^v K_v(\omega)\right\}. \qquad (A.13)$$

In a similar spirit to the representation of d^l_{mn}, these are represented as structures of the form

$$\sum_j a_j \omega^{p_j} K_{o_j}(\omega) \qquad (A.14)$$

in which we keep track of a_j, p_j, and o_j. Derivatives are added to the representation using (41)

$$\dot{K}_v(\omega) = -K_{v-1}(\omega) - \frac{v}{\omega} K_v(\omega) \qquad (A.15)$$

The final step is evaluation of structures such as Eq. A.14 at particular frequencies ω. Numerical stability of the final formulas is greatly improved by replacing higher order Bessel functions with lower order ones using the usual identities. (41)

TABLE I. Electrostatic moments for H_2O, H_2

Molecule	Mulitipole	Reference
H_2O	$\mu=1.8549 \times 10^{-18}$ esu	24
	$\Phi_{xx}=-0.13 \times 10^{-26}$ esu	24
	$\Phi_{yy}=-2.5 \times 10^{-26}$ esu	24
	$\Phi_{zz}=2.63 \times 10^{-26}$ esu	24
H_2	$\Theta_{zz}=-0.616 \times 10^{-26}$ esu	25

TABLE II. Atom-atom Lennard-Jones (6-12) parameters

Pair	ε/K	σ/Angstrom
H-N	20.5	3.0
C-N	34.3	3.45
Isotropic	119.3	3.838

TABLE III. Calculated Half-Widths for H_2O Broadened by H_2 at 296 K

J'	Ka'	Kc'	J"	Ka"	Kc"	γ†	J'	Ka'	Kc'	J"	Ka"	Kc"	γ†
1	0	1	0	0	0	0.103	4	3	2	3	0	3	0.091
1	1	1	0	0	0	0.101	3	2	1	3	1	2	0.093
1	1	0	1	0	1	0.096	3	3	1	3	1	2	0.090
2	0	2	1	0	1	0.097	4	1	3	3	1	2	0.093
2	1	2	1	0	1	0.097	4	2	3	3	1	2	0.089
2	2	0	1	0	1	0.098	4	3	1	3	1	2	0.090
2	1	1	1	1	0	0.096	4	4	1	3	1	2	0.089
2	2	1	1	1	0	0.090	3	1	2	3	1	3	0.093
1	1	0	1	1	1	0.097	3	2	2	3	1	3	0.090
2	0	2	1	1	1	0.099	3	3	0	3	1	3	0.092
2	1	2	1	1	1	0.098	4	0	4	3	1	3	0.086
2	2	0	1	1	1	0.094	4	1	4	3	1	3	0.085
2	1	1	2	0	2	0.098	4	2	2	3	1	3	0.092
2	2	1	2	0	2	0.096	4	3	2	3	1	3	0.089
3	0	3	2	0	2	0.093	4	4	0	3	1	3	0.092
3	1	3	2	0	2	0.092	3	3	0	3	2	1	0.085
3	2	1	2	0	2	0.096	4	0	4	3	2	1	0.091
3	3	1	2	0	2	0.095	4	1	4	3	2	1	0.090
2	2	0	2	1	1	0.093	4	2	2	3	2	1	0.091
3	1	2	2	1	1	0.096	4	3	2	3	2	1	0.086
3	2	2	2	1	1	0.092	4	4	0	3	2	1	0.084
3	3	0	2	1	1	0.090	3	2	1	3	2	2	0.089
2	1	1	2	1	2	0.097	3	3	1	3	2	2	0.085
2	2	1	2	1	2	0.095	4	1	3	3	2	2	0.090
3	0	3	2	1	2	0.093	4	2	3	3	2	2	0.086
3	1	3	2	1	2	0.092	4	3	1	3	2	2	0.085
3	2	1	2	1	2	0.095	4	4	1	3	2	2	0.084
3	3	1	2	1	2	0.094	4	1	3	3	3	0	0.090
3	0	3	2	2	0	0.096	4	2	3	3	3	0	0.085
3	1	3	2	2	0	0.095	4	3	1	3	3	0	0.080
3	2	1	2	2	0	0.089	4	4	1	3	3	0	0.073
3	3	1	2	2	0	0.081	3	3	0	3	3	1	0.076
2	2	0	2	2	1	0.087	4	0	4	3	3	1	0.091
3	1	2	2	2	1	0.093	4	2	2	3	3	1	0.087
3	2	2	2	2	1	0.088	4	3	2	3	3	1	0.080
3	3	0	2	2	1	0.081	4	4	0	3	3	1	0.073
3	1	2	3	0	3	0.094	4	1	3	4	0	4	0.089
3	2	2	3	0	3	0.092	4	2	3	4	0	4	0.085
3	3	0	3	0	3	0.093	4	3	1	4	0	4	0.089
4	0	4	3	0	3	0.087	5	0	5	4	0	4	0.080
4	1	4	3	0	3	0.086	5	1	5	4	0	4	0.080
4	2	2	3	0	3	0.093	5	2	3	4	0	4	0.090

† in units of cm^{-1}/atm.

TABLE III. Calculated Half-Widths for H_2O Broadened by H_2 at 296 K

J'	Ka'	Kc'	J"	Ka"	Kc"	γ†		J'	Ka'	Kc'	J"	Ka"	Kc"	γ†
5	3	3	4	0	4	0.085		5	4	1	4	3	2	0.079
4	2	2	4	1	3	0.091		5	5	1	4	3	2	0.079
4	3	2	4	1	3	0.088		5	3	3	4	4	0	0.080
4	4	0	4	1	3	0.088		5	4	1	4	4	0	0.075
5	1	4	4	1	3	0.089		5	5	1	4	4	0	0.069
5	2	4	4	1	3	0.086		4	4	0	4	4	1	0.070
5	3	2	4	1	3	0.089		5	1	4	4	4	1	0.087
5	4	2	4	1	3	0.087		5	3	2	4	4	1	0.081
4	1	3	4	1	4	0.088		5	4	2	4	4	1	0.075
4	2	3	4	1	4	0.084		5	5	0	4	4	1	0.069
4	3	1	4	1	4	0.088		5	1	4	5	0	5	0.083
4	4	1	4	1	4	0.090		5	2	4	5	0	5	0.080
5	0	5	4	1	4	0.079		5	3	2	5	0	5	0.085
5	1	5	4	1	4	0.078		6	0	6	5	0	5	0.074
5	2	3	4	1	4	0.089		6	1	6	5	0	5	0.074
5	3	3	4	1	4	0.084		6	2	4	5	0	5	0.086
5	4	1	4	1	4	0.087		6	3	4	5	0	5	0.081
4	3	1	4	2	2	0.087		5	2	3	5	1	4	0.089
4	4	1	4	2	2	0.086		5	3	3	5	1	4	0.084
5	0	5	4	2	2	0.088		5	4	1	5	1	4	0.085
5	1	5	4	2	2	0.087		6	1	5	5	1	4	0.084
5	2	3	4	2	2	0.091		6	2	5	5	1	4	0.082
5	3	3	4	2	2	0.086		6	3	3	5	1	4	0.087
5	4	1	4	2	2	0.085		6	4	3	5	1	4	0.084
4	2	2	4	2	3	0.087		6	6	1	5	1	4	0.092
4	3	2	4	2	3	0.083		5	1	4	5	1	5	0.083
5	1	4	4	2	3	0.085		5	2	4	5	1	5	0.079
5	2	4	4	2	3	0.082		5	3	2	5	1	5	0.085
5	3	2	4	2	3	0.084		5	4	2	5	1	5	0.085
5	4	2	4	2	3	0.083		6	0	6	5	1	5	0.073
4	4	0	4	3	1	0.079		6	1	6	5	1	5	0.073
5	1	4	4	3	1	0.087		6	2	4	5	1	5	0.085
5	2	4	4	3	1	0.083		6	3	4	5	1	5	0.080
5	3	2	4	3	1	0.083		6	4	2	5	1	5	0.084
5	4	2	4	3	1	0.080		5	3	2	5	2	3	0.088
5	5	0	4	3	1	0.079		5	4	2	5	2	3	0.086
4	3	1	4	3	2	0.082		6	0	6	5	2	3	0.085
4	4	1	4	3	2	0.078		6	1	6	5	2	3	0.085
5	0	5	4	3	2	0.086		6	2	4	5	2	3	0.090
5	1	5	4	3	2	0.085		6	3	4	5	2	3	0.085
5	2	3	4	3	2	0.087		6	4	2	5	2	3	0.086
5	3	3	4	3	2	0.081		6	5	2	5	2	3	0.087

† in units of cm^{-1}/atm.

TABLE III. Calculated Half-Widths for H₂O Broadened by H₂ at 296 K

J'	Ka'	Kc'	J"	Ka"	Kc"	γ†	J'	Ka'	Kc'	J"	Ka"	Kc"	γ†
5	2	3	5	2	4	0.086	7	0	7	6	0	6	0.069
5	3	3	5	2	4	0.080	7	1	7	6	0	6	0.069
6	1	5	5	2	4	0.080	7	2	5	6	0	6	0.082
6	2	5	5	2	4	0.078	7	3	5	6	0	6	0.077
6	3	3	5	2	4	0.083	6	2	4	6	1	5	0.086
6	4	3	5	2	4	0.080	6	3	4	6	1	5	0.081
5	4	1	5	3	2	0.081	6	4	2	6	1	5	0.083
6	1	5	5	3	2	0.084	7	1	6	6	1	5	0.079
6	2	5	5	3	2	0.082	7	2	6	6	1	5	0.078
6	3	3	5	3	2	0.085	7	3	4	6	1	5	0.085
6	4	3	5	3	2	0.081	7	4	4	6	1	5	0.081
6	5	1	5	3	2	0.082	6	1	5	6	1	6	0.078
6	6	1	5	3	2	0.085	6	2	5	6	1	6	0.075
5	3	2	5	3	3	0.082	6	4	3	6	1	6	0.081
5	4	2	5	3	3	0.079	7	0	7	6	1	6	0.069
5	5	0	5	3	3	0.081	7	1	7	6	1	6	0.069
6	0	6	5	3	3	0.081	7	2	5	6	1	6	0.082
6	2	4	5	3	3	0.085	7	3	5	6	1	6	0.077
6	3	4	5	3	3	0.079	7	4	3	6	1	6	0.082
6	4	2	5	3	3	0.080	6	3	3	6	2	4	0.088
6	5	2	5	3	3	0.080	6	4	3	6	2	4	0.084
5	5	0	5	4	1	0.075	7	1	7	6	2	4	0.083
6	2	4	5	4	1	0.085	7	2	5	6	2	4	0.088
6	3	4	5	4	1	0.080	7	3	5	6	2	4	0.083
6	4	2	5	4	1	0.078	7	4	3	6	2	4	0.085
6	5	2	5	4	1	0.077	6	2	4	6	2	5	0.084
5	4	1	5	4	2	0.077	6	3	4	6	2	5	0.078
5	5	1	5	4	2	0.075	6	4	2	6	2	5	0.080
6	1	5	5	4	2	0.084	7	1	6	6	2	5	0.076
6	3	3	5	4	2	0.083	7	2	6	6	2	5	0.075
6	4	3	5	4	2	0.078	7	3	4	6	2	5	0.083
6	5	1	5	4	2	0.077	7	4	4	6	2	5	0.079
6	4	3	5	5	0	0.078	7	5	2	6	2	5	0.081
6	5	1	5	5	0	0.074	6	4	2	6	3	3	0.083
6	6	1	5	5	0	0.070	7	1	6	6	3	3	0.083
5	5	0	5	5	1	0.069	7	2	6	6	3	3	0.082
6	4	2	5	5	1	0.078	7	3	4	6	3	3	0.086
6	5	2	5	5	1	0.074	7	4	4	6	3	3	0.082
6	6	0	5	5	1	0.070	7	5	2	6	3	3	0.083
6	1	5	6	0	6	0.078	6	3	3	6	3	4	0.082
6	2	5	6	0	6	0.075	6	4	3	6	3	4	0.079
6	3	3	6	0	6	0.083	6	6	1	6	3	4	0.084

† in units of cm⁻¹/atm.

TABLE III. Calculated Half-Widths for H_2O Broadened by H_2 at 296 K

J'	Ka'	Kc'	J"	Ka"	Kc"	γ†		J'	Ka'	Kc'	J"	Ka"	Kc"	γ†
7	0	7	6	3	4	0.078		8	1	7	7	1	6	0.074
7	2	5	6	3	4	0.082		8	2	7	7	1	6	0.073
7	3	5	6	3	4	0.078		8	3	5	7	1	6	0.082
7	4	3	6	3	4	0.080		8	4	5	7	1	6	0.078
7	5	3	6	3	4	0.080		7	1	6	7	1	7	0.073
6	5	1	6	4	2	0.078		7	2	6	7	1	7	0.072
7	3	5	6	4	2	0.079		8	0	8	7	1	7	0.066
7	4	3	6	4	2	0.080		8	1	8	7	1	7	0.066
7	5	3	6	4	2	0.079		8	2	6	7	1	7	0.078
6	4	2	6	4	3	0.078		7	3	4	7	2	5	0.086
6	5	2	6	4	3	0.078		7	4	4	7	2	5	0.082
7	1	6	6	4	3	0.080		7	5	2	7	2	5	0.084
7	3	4	6	4	3	0.083		8	1	8	7	2	5	0.080
7	4	4	6	4	3	0.078		8	2	6	7	2	5	0.084
7	5	2	6	4	3	0.078		8	3	6	7	2	5	0.080
6	6	0	6	5	1	0.076		8	4	4	7	2	5	0.084
7	4	4	6	5	1	0.079		8	5	4	7	2	5	0.083
7	5	2	6	5	1	0.078		7	2	5	7	2	6	0.081
7	6	2	6	5	1	0.077		7	3	5	7	2	6	0.076
6	5	1	6	5	2	0.076		7	4	3	7	2	6	0.079
6	6	1	6	5	2	0.076		8	1	7	7	2	6	0.072
7	4	3	6	5	2	0.080		8	2	7	7	2	6	0.072
7	5	3	6	5	2	0.078		8	3	5	7	2	6	0.081
7	6	1	6	5	2	0.077		8	4	5	7	2	6	0.076
7	5	3	6	6	0	0.079		7	4	3	7	3	4	0.084
7	6	1	6	6	0	0.075		8	1	7	7	3	4	0.081
7	7	1	6	6	0	0.070		8	2	7	7	3	4	0.081
6	6	0	6	6	1	0.071		8	3	5	7	3	4	0.086
7	3	4	6	6	1	0.088		8	4	5	7	3	4	0.082
7	5	2	6	6	1	0.079		8	5	3	7	3	4	0.083
7	6	2	6	6	1	0.075		7	3	4	7	3	5	0.082
7	7	0	6	6	1	0.070		7	4	4	7	3	5	0.078
7	1	6	7	0	7	0.073		7	5	2	7	3	5	0.080
7	2	6	7	0	7	0.072		8	0	8	7	3	5	0.075
7	3	4	7	0	7	0.082		8	2	6	7	3	5	0.079
8	0	8	7	0	7	0.066		8	3	6	7	3	5	0.076
8	1	8	7	0	7	0.066		8	4	4	7	3	5	0.080
8	2	6	7	0	7	0.078		8	5	4	7	3	5	0.079
8	3	6	7	0	7	0.074		7	5	2	7	4	3	0.080
7	2	5	7	1	6	0.082		8	2	6	7	4	3	0.082
7	3	5	7	1	6	0.077		8	3	6	7	4	3	0.078
7	4	3	7	1	6	0.080		8	4	4	7	4	3	0.081

† in units of cm⁻¹/atm.

TABLE III. Calculated Half-Widths for H_2O Broadened by H_2 at 296 K

J'	Ka'	Kc'	J"	Ka"	Kc"	γ†		J'	Ka'	Kc'	J"	Ka"	Kc"	γ†
8	5	4	7	4	3	0.079		9	4	6	8	1	7	0.075
7	4	3	7	4	4	0.079		8	1	7	8	1	8	0.069
7	5	3	7	4	4	0.078		8	2	7	8	1	8	0.069
8	1	7	7	4	4	0.077		9	0	9	8	1	8	0.063
8	3	5	7	4	4	0.082		9	1	9	8	1	8	0.063
8	4	5	7	4	4	0.077		9	2	7	8	1	8	0.073
8	5	3	7	4	4	0.078		9	3	7	8	1	8	0.071
7	6	1	7	5	2	0.079		8	3	5	8	2	6	0.084
8	4	5	7	5	2	0.079		8	4	5	8	2	6	0.079
8	5	3	7	5	2	0.079		8	5	3	8	2	6	0.081
8	6	3	7	5	2	0.078		9	1	9	8	2	6	0.076
7	5	2	7	5	3	0.078		9	2	7	8	2	6	0.079
7	6	2	7	5	3	0.079		9	3	7	8	2	6	0.077
8	4	4	7	5	3	0.081		9	4	5	8	2	6	0.082
8	5	4	7	5	3	0.078		9	5	5	8	2	6	0.080
8	6	2	7	5	3	0.078		8	2	6	8	2	7	0.077
7	7	0	7	6	1	0.076		8	3	6	8	2	7	0.073
8	5	4	7	6	1	0.080		9	1	8	8	2	7	0.069
8	6	2	7	6	1	0.078		9	2	8	8	2	7	0.069
8	7	2	7	6	1	0.076		9	3	6	8	2	7	0.079
7	6	1	7	6	2	0.077		9	4	6	8	2	7	0.074
7	7	1	7	6	2	0.076		8	4	4	8	3	5	0.084
8	5	3	7	6	2	0.080		9	2	8	8	3	5	0.079
8	6	3	7	6	2	0.078		9	3	6	8	3	5	0.085
8	7	1	7	6	2	0.076		9	4	6	8	3	5	0.081
8	6	3	7	7	0	0.078		8	3	5	8	3	6	0.080
8	7	1	7	7	0	0.073		8	4	5	8	3	6	0.076
8	8	1	7	7	0	0.068		9	0	9	8	3	6	0.072
7	7	0	7	7	1	0.070		9	2	7	8	3	6	0.075
8	7	2	7	7	1	0.073		9	3	7	8	3	6	0.073
8	8	0	7	7	1	0.068		9	4	5	8	3	6	0.079
8	1	7	8	0	8	0.069		9	5	5	8	3	6	0.076
8	2	7	8	0	8	0.069		9	6	3	8	3	6	0.077
8	3	5	8	0	8	0.081		8	5	3	8	4	4	0.080
9	0	9	8	0	8	0.063		9	1	9	8	4	4	0.079
9	1	9	8	0	8	0.063		9	3	7	8	4	4	0.078
9	3	7	8	0	8	0.071		9	4	5	8	4	4	0.082
8	2	6	8	1	7	0.077		9	5	5	8	4	4	0.079
8	3	6	8	1	7	0.073		8	4	4	8	4	5	0.079
8	4	4	8	1	7	0.079		8	5	4	8	4	5	0.078
9	1	8	8	1	7	0.069		9	1	8	8	4	5	0.075
9	2	8	8	1	7	0.069		9	3	6	8	4	5	0.080

† in units of cm^{-1}/atm.

TABLE III. Calculated Half-Widths for H_2O Broadened by H_2 at 296 K

J'	Ka'	Kc'	J"	Ka"	Kc"	γ†		J'	Ka'	Kc'	J"	Ka"	Kc"	γ†
9	4	6	8	4	5	0.076		10	0	10	9	1	9	0.061
9	5	4	8	4	5	0.077		10	1	10	9	1	9	0.061
8	6	2	8	5	3	0.078		10	2	8	9	1	9	0.070
9	4	6	8	5	3	0.078		9	3	6	9	2	7	0.080
9	5	4	8	5	3	0.078		9	4	6	9	2	7	0.076
9	6	4	8	5	3	0.077		9	5	4	9	2	7	0.078
8	5	3	8	5	4	0.078		10	1	10	9	2	7	0.072
8	6	3	8	5	4	0.078		10	2	8	9	2	7	0.074
9	4	5	8	5	4	0.080		10	3	8	9	2	7	0.073
9	5	5	8	5	4	0.077		10	5	6	9	2	7	0.076
9	6	3	8	5	4	0.077		9	2	7	9	2	8	0.073
8	7	1	8	6	2	0.077		9	3	7	9	2	8	0.070
9	5	5	8	6	2	0.078		10	1	9	9	2	8	0.066
9	6	3	8	6	2	0.077		10	2	9	9	2	8	0.066
9	7	3	8	6	2	0.076		10	3	7	9	2	8	0.076
8	6	2	8	6	3	0.077		9	4	5	9	3	6	0.083
8	7	2	8	6	3	0.077		10	2	9	9	3	6	0.077
9	5	4	8	6	3	0.078		10	3	7	9	3	6	0.082
9	6	4	8	6	3	0.077		10	4	7	9	3	6	0.079
9	7	2	8	6	3	0.076		9	3	6	9	3	7	0.078
8	8	0	8	7	1	0.072		9	4	6	9	3	7	0.074
9	8	2	8	7	1	0.072		10	2	8	9	3	7	0.072
8	7	1	8	7	2	0.074		10	3	8	9	3	7	0.071
8	8	1	8	7	2	0.072		10	4	6	9	3	7	0.077
9	6	3	8	7	2	0.077		9	5	4	9	4	5	0.080
9	7	3	8	7	2	0.074		10	3	8	9	4	5	0.077
9	8	1	8	7	2	0.072		10	4	6	9	4	5	0.082
8	8	0	8	8	1	0.066		10	5	6	9	4	5	0.079
9	9	0	8	8	1	0.062		9	4	5	9	4	6	0.079
9	1	8	9	0	9	0.066		9	5	5	9	4	6	0.076
9	2	8	9	0	9	0.066		10	3	7	9	4	6	0.078
10	0	10	9	0	9	0.061		10	4	7	9	4	6	0.074
10	1	10	9	0	9	0.061		10	5	5	9	4	6	0.076
10	3	8	9	0	9	0.069		9	6	3	9	5	4	0.077
9	2	7	9	1	8	0.073		10	4	7	9	5	4	0.076
9	3	7	9	1	8	0.070		10	5	5	9	5	4	0.077
9	4	5	9	1	8	0.078		10	6	5	9	5	4	0.076
10	1	9	9	1	8	0.066		9	5	4	9	5	5	0.077
10	2	9	9	1	8	0.066		9	6	4	9	5	5	0.077
10	4	7	9	1	8	0.072		10	4	6	9	5	5	0.080
9	1	8	9	1	9	0.066		10	5	6	9	5	5	0.076
9	2	8	9	1	9	0.066		10	6	4	9	5	5	0.076

† in units of cm⁻¹/atm.

TABLE III. Calculated Half-Widths for H_2O Broadened by H_2 at 296 K

J'	Ka'	Kc'	J"	Ka"	Kc"	γ†	J'	Ka'	Kc'	J"	Ka"	Kc"	γ†
9	7	2	9	6	3	0.076	11	4	7	10	3	8	0.076
10	5	6	9	6	3	0.076	10	5	5	10	4	6	0.080
10	6	4	9	6	3	0.075	11	3	9	10	4	6	0.077
10	7	4	9	6	3	0.074	11	4	7	10	4	6	0.080
9	6	3	9	6	4	0.076	11	5	7	10	4	6	0.078
9	7	3	9	6	4	0.076	10	4	6	10	4	7	0.078
10	5	5	9	6	4	0.077	10	5	6	10	4	7	0.075
10	6	5	9	6	4	0.075	11	3	8	10	4	7	0.075
10	7	3	9	6	4	0.074	11	4	8	10	4	7	0.073
9	8	1	9	7	2	0.073	11	5	6	10	4	7	0.075
10	6	5	9	7	2	0.076	10	6	4	10	5	5	0.076
10	8	3	9	7	2	0.072	11	4	8	10	5	5	0.075
9	7	2	9	7	3	0.074	11	6	6	10	5	5	0.075
9	8	2	9	7	3	0.073	10	5	5	10	5	6	0.076
10	1	9	10	0	10	0.064	10	6	5	10	5	6	0.075
10	2	9	10	0	10	0.064	11	4	7	10	5	6	0.078
11	0	11	10	0	10	0.059	11	5	7	10	5	6	0.074
11	1	11	10	0	10	0.059	11	6	5	10	5	6	0.074
10	2	8	10	1	9	0.069	10	7	3	10	6	4	0.074
10	2	8	10	1	9	0.069	10	7	4	10	6	5	0.074
10	3	8	10	1	9	0.068	11	5	6	10	6	5	0.076
11	1	10	10	1	9	0.065	11	7	4	10	6	5	0.072
10	1	9	10	1	10	0.064	10	8	3	10	7	4	0.071
10	2	9	10	1	10	0.064	11	1	10	11	0	11	0.062
11	0	11	10	1	10	0.059	12	0	12	11	0	11	0.058
11	0	11	10	1	10	0.059	12	1	12	11	0	11	0.058
11	1	11	10	1	10	0.059	11	2	9	11	1	10	0.067
11	2	9	10	1	10	0.067	12	1	11	11	1	10	0.064
10	3	7	10	2	8	0.076	12	2	11	11	1	10	0.064
11	2	9	10	2	8	0.070	11	2	10	11	1	11	0.062
11	3	9	10	2	8	0.070	12	0	12	11	1	11	0.058
10	2	8	10	2	9	0.069	12	1	12	11	1	11	0.058
10	3	8	10	2	9	0.068	11	3	8	11	2	9	0.073
11	1	10	10	2	9	0.065	12	2	10	11	2	9	0.068
11	2	10	10	2	9	0.064	12	3	10	11	2	9	0.068
11	3	8	10	2	9	0.073	11	3	9	11	2	10	0.067
10	4	6	10	3	7	0.081	12	1	11	11	2	10	0.064
11	3	8	10	3	7	0.078	12	2	11	11	2	10	0.064
11	4	8	10	3	7	0.076	11	4	7	11	3	8	0.078
10	3	7	10	3	8	0.076	12	3	9	11	3	8	0.075
10	4	7	10	3	8	0.072	12	4	9	11	3	8	0.074
11	3	9	10	3	8	0.069	11	4	8	11	3	9	0.071

† in units of cm^{-1}/atm.

TABLE III. Calculated Half-Widths for H_2O Broadened by H_2 at 296 K

J'	Ka'	Kc'	J"	Ka"	Kc"	γ †
12	2	10	11	3	9	0.068
12	3	10	11	3	9	0.068
11	5	6	11	4	7	0.078
12	5	8	11	4	7	0.076
11	5	7	11	4	8	0.073
12	3	9	11	4	8	0.073
11	6	5	11	5	6	0.075
12	4	9	11	5	6	0.075
12	6	7	11	5	6	0.074
11	6	6	11	5	7	0.073
11	7	4	11	6	5	0.072
12	1	11	12	0	12	0.062
13	0	13	12	0	12	0.058
13	1	13	12	0	12	0.058
12	2	10	12	1	11	0.066
13	1	12	12	1	11	0.063
13	2	12	12	1	11	0.063
12	2	11	12	1	12	0.062
13	0	13	12	1	12	0.058
13	1	13	12	1	12	0.058
12	3	9	12	2	10	0.071
13	3	11	12	2	10	0.068
12	3	10	12	2	11	0.066
13	1	12	12	2	11	0.063
13	2	12	12	2	11	0.063
12	4	8	12	3	9	0.075
12	4	9	12	3	10	0.070
13	2	11	12	3	10	0.068
12	5	7	12	4	8	0.076
12	5	8	12	4	9	0.072
13	3	10	12	4	9	0.072
12	6	7	12	5	8	0.071
13	1	12	13	0	13	0.062
14	0	14	13	0	13	0.053
14	1	14	13	0	13	0.059
13	2	11	13	1	12	0.066
13	4	9	13	3	10	0.074
13	5	8	13	4	9	0.074

† in units of cm^{-1}/atm.

TABLE IV. Measured and Calculated Half-Widths for the 22GHz line

Temperature K	Measured†	Ref.	Calculated†	% Error
293	0.0710 (±.0.0076)	7	0.085	-20.
300	0.0834 (±.0.0021)	6	0.084	-0.72

† in units of cm⁻¹/atm.

TABLE V.   Calculated Temperature Exponents for H_2O Broadened by H_2

J'	Ka'	Kc'	J"	Ka"	Kc"	γ(200 K)†	γ(200 K)†	γ(200 K)†	γ(200 K)†	n
2	2	1	1	1	0	0.108	0.098	0.090	0.077	0.50
2	2	0	2	1	1	0.114	0.102	0.093	0.078	0.54
4	1	4	3	2	1	0.108	0.098	0.090	0.077	0.48
5	3	2	4	2	3	0.098	0.090	0.084	0.073	0.43
6	1	6	5	2	3	0.101	0.092	0.085	0.073	0.47
6	1	6	5	0	5	0.081	0.077	0.074	0.066	0.29
6	2	5	5	1	4	0.095	0.088	0.082	0.071	0.42
6	2	4	5	1	5	0.101	0.092	0.085	0.074	0.46
6	3	4	5	2	3	0.101	0.092	0.085	0.073	0.47
6	3	3	5	2	4	0.098	0.090	0.083	0.072	0.44
6	4	3	5	3	2	0.095	0.087	0.081	0.070	0.43
6	4	2	5	3	3	0.092	0.085	0.080	0.070	0.40
6	5	2	5	4	1	0.089	0.082	0.077	0.067	0.41
6	5	1	5	4	2	0.089	0.082	0.077	0.067	0.41
6	6	1	5	5	0	0.083	0.075	0.070	0.061	0.44
6	6	0	5	5	1	0.083	0.075	0.070	0.061	0.44
7	5	3	6	4	2	0.094	0.085	0.079	0.068	0.46
8	6	3	7	5	2	0.098	0.086	0.078	0.066	0.56
9	7	3	8	6	2	0.097	0.084	0.076	0.065	0.59
10	8	3	9	7	2	0.088	0.078	0.072	0.062	0.50

† in units of cm^{-1}/atm.

Table VI. Measured Halfwidths of H_2O broadening by He and Temperature Dependence

Transition						$\gamma\dagger \times 10^3$	T /K	n	Ref.
3	1	3	2	2	0	21.7±0.2	300.	0.39±0.10	9
3	1	3	2	2	0	21.4±0.2	315.	0.39±0.10	9
3	1	3	2	2	0	21.1±0.2	330.	0.39±0.10	9
3	1	3	2	2	0	20.4±0.2	360.	0.39±0.10	9
3	1	3	2	2	0	20.1±0.2	375.	0.39±0.10	9
3	1	3	2	2	0	19.6±0.3	390.	0.39±0.10	9
4	1	4	3	2	1	20.3±0.2	300.	0.34±0.09	9
4	1	4	3	2	1	19.8±0.2	324.	0.34±0.09	9
4	1	4	3	2	1	19.3±0.2	348.	0.34±0.09	9
4	1	4	3	2	1	18.9±0.2	373.	0.34±0.09	9
6	1	6	5	2	3	24.6±0.5	300.		6
6	1	6	5	2	3	20.0±1.3	293.		7
3	1	3	2	2	0	18.0±1.8	597.	0.49±0.02	10
3	1	3	2	2	0	20.3±2.0	444.	0.49±0.02	10
3	1	3	2	2	0	22.0±2.2	297.	0.49±0.02	10
3	1	3	2	2	0	24.1±2.4	264.	0.49±0.02	10
3	1	3	2	2	0	29.4±2.9	192.	0.49±0.02	10
3	1	3	2	2	0	32.2±3.2	177.	0.49±0.02	10
3	1	3	2	2	0	34.2±3.4	162.	0.49±0.02	10
3	1	3	2	2	0	37.2±3.7	144.	0.49±0.02	10
3	1	3	2	2	0	38.2±3.8	120.	0.49±0.02	10
3	1	3	2	2	0	40.5±4.0	104.	0.49±0.02	10
3	1	3	2	2	0	39.3±3.9	103.	0.49±0.02	10
3	1	3	2	2	0	44.1±4.4	87.	0.49±0.02	10
3	1	3	2	2	0	46.9±4.7	83.	0.49±0.02	10
6	6	1	5	3	2	50.0±25.0	353.		11
6	6	0	5	3	3	30.0±15.0	353.		11
7	6	1	6	3	4	50.0±25.0	353.		11
7	6	2	6	3	3	30.0±15.0	353.		11
8	6	3	7	3	4	80.0±40.0	353.		11
12	5	8	11	2	9	40.0±20.0	353.		11
13	4	9	12	3	10	50.0±25.0	353.		11

$\dagger$ in units of cm^{-1}/atm

Table VII. H_2O broadening by He, N_2, O_2, CO_2, and H_2 and the Ratio to the He-Broadened Value

Transition	$\gamma \times 10^3$ He†	$\gamma \times 10^3$ N_2†	Ratio	$\gamma \times 10^3$ O_2†	Ratio	$\gamma \times 10^3$ CO_2†	Ratio	$\gamma \times 10^3$ H_2†	Ratio
1	21.8	105.	0.21	69.6	0.31	157.	0.14	94.7	0.23
2	20.4	102.	0.20	67.1	0.30	152.	0.13	90.4	0.23
3	24.8	96.7	0.26	63.7	0.39	144.	0.17	85.0	0.29

† in units of cm^{-1}/atm

Figure 1   Calculated H_2-broadened halfwidth for the 22 GHz line of H_2O as a function of order, Q, of the atom-atom potential.   Open circles and solid squares correspond to T=293 and 300K.
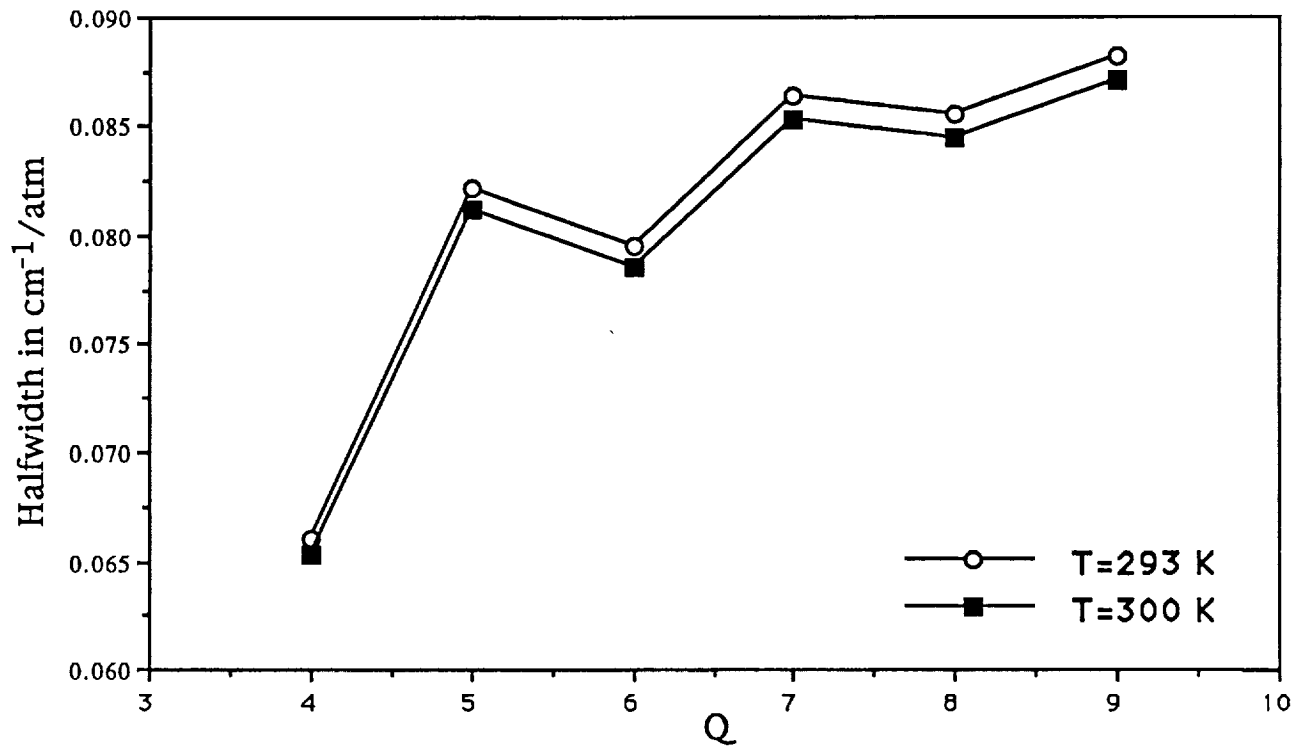
Figure 2   Percent difference calculated minus estimated halfwidth versus
            (J"+J')/2.   Solid squares and + symbol correspond to average
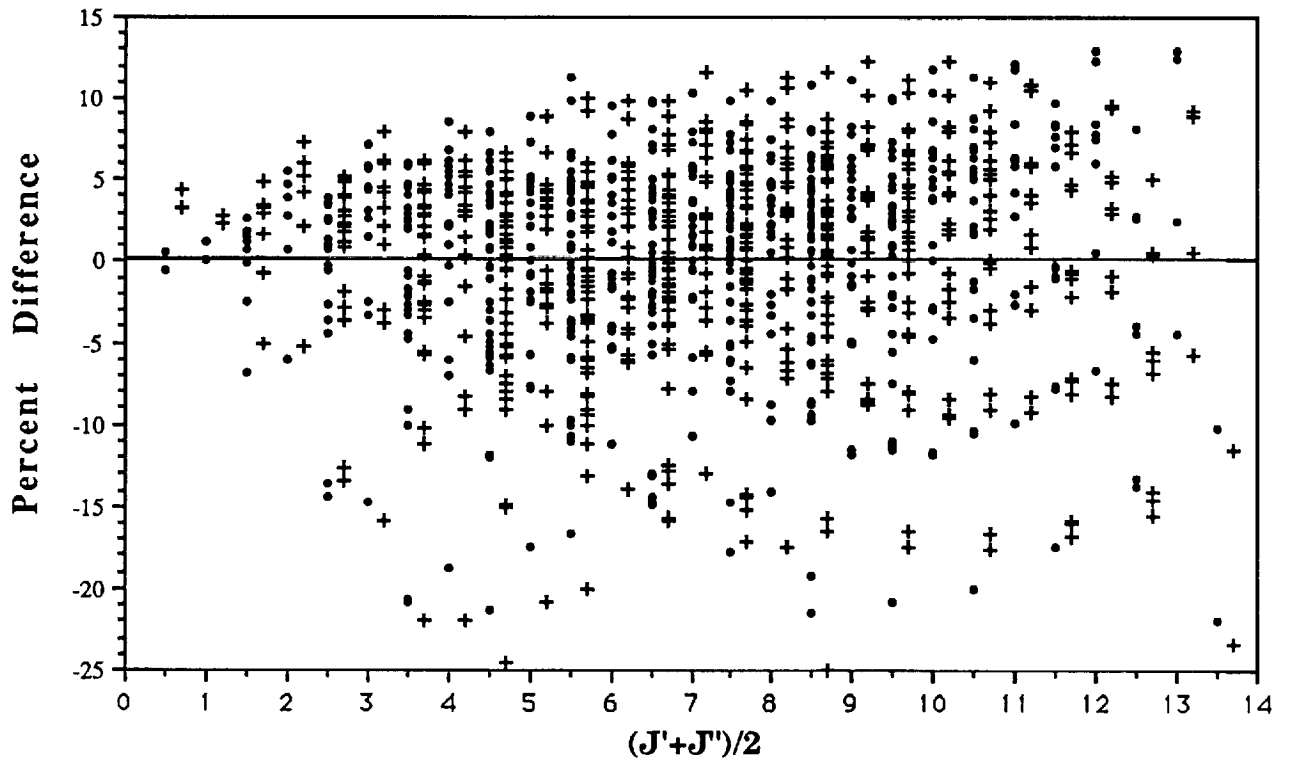   and polynomial method respectively.

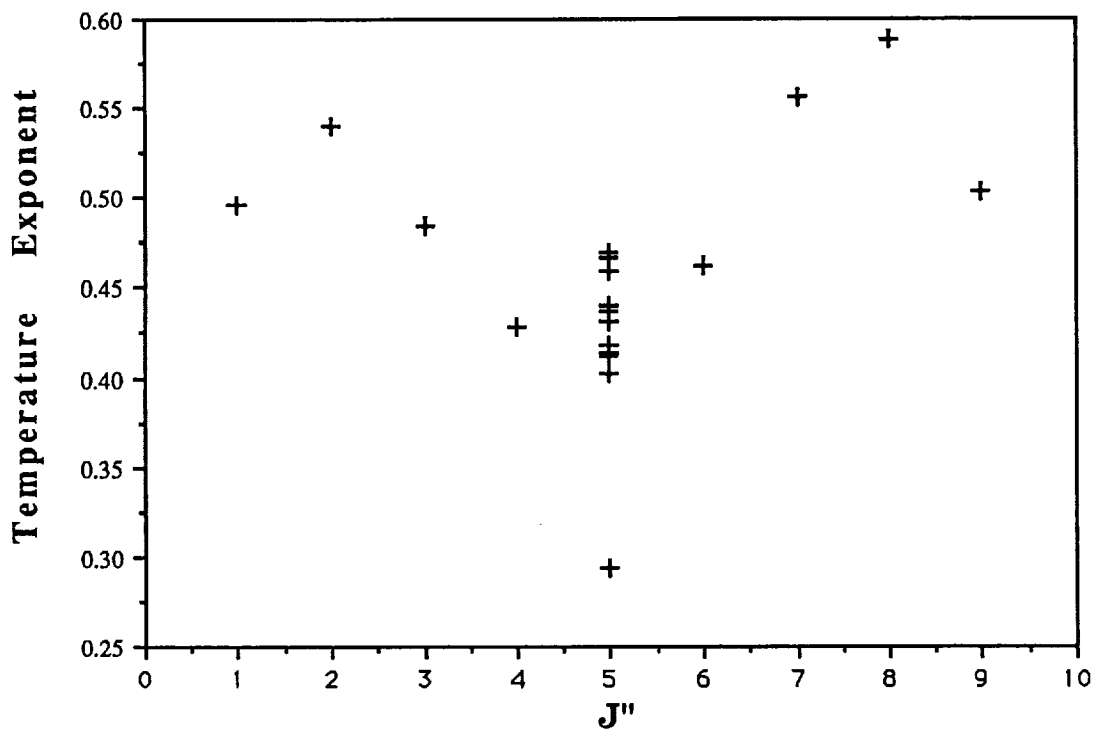Figure 3.   Calculated temperature exponents (see Table V) versus J".

Figure 4. Calculated temperature exponents (see Table V) versus Ka" for transitions with J"=5.

$J''(J''+1)+Ka''-Kc''+1$